

801 **A Proofs**

802 **A.1 Proof of Theorem 3**

803 First, we define the empirical post-processing gap

$$\text{pGap}(f, S) := \frac{1}{n} \sum_{i=1}^n \ell_{\text{sq}}(f(X_i), Y_i) - \inf_{h \in \text{Lip}_{L=1}} \frac{1}{n} \sum_{i=1}^n \ell_{\text{sq}}(f(X_i) + h(f(X_i)), Y_i).$$

804 We can prove that

$$\text{smCE}(f, S)^2 \leq \text{pGap}(f, S) \leq 2\text{smCE}(f, S).$$

805 The proof follows directly from Lemma 4.7 in Błasik et al. [3], with the only modification of
806 replacing the population expectation under \mathcal{D} with the empirical expectation in the last step of their
807 proof.

808 Accordingly, we upper bound the empirical post-processing gap using the L_2 -regularized ERM
809 objective evaluated at f and $f + h \circ f$. For notational simplicity, we denote ℓ_{sq} by ℓ and write
810 $r \circ f := f + h \circ f$.

811 Then we have

$$\begin{aligned} & \text{pGap}(f, S) \\ &= \frac{1}{n} \sum_{i=1}^n \ell(f(X_i), Y_i) - \inf_{h \in \text{Lip}_{L=1}} \frac{1}{n} \sum_{i=1}^n \ell(r \circ f(X_i), Y_i) \\ &= \frac{1}{n} \sum_{i=1}^n \ell(f(X_i), Y_i) + \lambda \|f\|_{\mathcal{F}}^2 - \lambda \|f\|_{\mathcal{F}}^2 - \inf_{h \in \text{Lip}_{L=1}} \frac{1}{n} \sum_{i=1}^n \ell(r \circ f(X_i), Y_i) \\ &= \frac{1}{n} \sum_{i=1}^n \ell(f(X_i), Y_i) + \lambda \|f\|_{\mathcal{F}}^2 - \lambda \|f\|_{\mathcal{F}}^2 - \inf_{h \in \text{Lip}_{L=1}} \left(\frac{1}{n} \sum_{i=1}^n \ell(r \circ f(X_i), Y_i) + \lambda \|r \circ f\|_{\mathcal{F}}^2 - \lambda \|r \circ f\|_{\mathcal{F}}^2 \right) \\ &= L_n(f) - \inf_{h \in \text{Lip}_{L=1}} \left(\frac{1}{n} \sum_{i=1}^n \ell(r \circ f(X_i), Y_i) + \lambda \|r \circ f\|_{\mathcal{F}}^2 + \lambda \|f\|_{\mathcal{F}}^2 - \lambda \|r \circ f\|_{\mathcal{F}}^2 \right) \\ &\leq L_n(f) - \inf_{h \in \text{Lip}_{L=1}} \left(\frac{1}{n} \sum_{i=1}^n \ell(r \circ f(X_i), Y_i) + \lambda \|r \circ f\|_{\mathcal{F}}^2 \right) - \inf_{h \in \text{Lip}_{L=1}} (\lambda \|f\|_{\mathcal{F}}^2 - \lambda \|r \circ f\|_{\mathcal{F}}^2) \\ &\leq L_n(f_n^*) + \text{err}_n(f) - \inf_{h \in \text{Lip}_{L=1}} \left(\frac{1}{n} \sum_{i=1}^n \ell(r \circ f(X_i), Y_i) + \lambda \|r \circ f\|_{\mathcal{F}}^2 \right) + 2\lambda \\ &= L_n(f_n^*) + \text{err}_n(f) - \inf_{h \in \text{Lip}_{L=1}} L_n(r \circ f) + 2\lambda \\ &\leq \text{err}_n(f) + 2\lambda, \end{aligned}$$

812 where we used that $L_n(f) = L_n(f_n^*) + \text{err}_n(f)$ and

$$\|r \circ f\|_{\mathcal{F}}^2 - \|f\|_{\mathcal{F}}^2 = (\|r \circ f\|_{\mathcal{F}} + \|f\|_{\mathcal{F}})(\|r \circ f\|_{\mathcal{F}} - \|f\|_{\mathcal{F}}) \leq 2\|r \circ f - f\|_{\mathcal{F}} \leq 2,$$

813 which is a direct consequence of the assumption on the norm of \mathcal{F} . In the final line, we also used the
814 following relation:

$$L_n(f_n^*) \leq \inf_{h \in \text{Lip}_{L=1}} L_n(r \circ f)$$

815 since f_n^* minimizes $L_n(f)$ over \mathcal{F} and we assume $f + h \circ f \in \mathcal{F}$.

816 **A.2 Proof of Theorem 4**

817 *Proof.* We follow the proof technique of Theorem 9.5 in Błasiok et al. [2];

$$\begin{aligned}
& \text{smCE}(f, \mathcal{D}) - \text{smCE}(f, S) \\
&= \sup_{\eta} \mathbb{E} \eta(f(X)) \cdot (Y - f(X)) - \sup'_{\eta} \frac{1}{n} \sum_i \eta'(f(X_i)) \cdot (Y_i - f(X_i)) \\
&= \sup_{\eta} \mathbb{E} \left[\frac{1}{2} (Y - (f - \eta(f)))^2 - \frac{1}{2} (Y - f)^2 - \frac{1}{2} \eta(f)^2 \right] \\
&\quad - \sup'_{\eta} \frac{1}{n} \sum_i \left[\frac{1}{2} (Y_i - (f_i - \eta'(f_i)))^2 - \frac{1}{2} (Y - f_i)^2 - \frac{1}{2} \eta'(f_i)^2 \right] \\
&\leq \sup_{\eta} \left(\mathbb{E} \left[\frac{1}{2} (Y - (f - \eta(f)))^2 - \frac{1}{2} (Y - f)^2 - \frac{1}{2} \eta(f)^2 \right] \right. \\
&\quad \left. - \frac{1}{n} \sum_i \left[\frac{1}{2} (Y_i - (f_i - \eta(f_i)))^2 - \frac{1}{2} (Y - f_i)^2 - \frac{1}{2} \eta(f_i)^2 \right] \right)
\end{aligned}$$

818 and then we take the supremum for f ,

$$\begin{aligned}
& \sup_{f \in \mathcal{F}} \text{smCE}(f, \mathcal{D}) - \text{smCE}(f, S) \\
&\leq \sup_{f \in \mathcal{F}} \sup_{\eta} \left(\mathbb{E} \left[\frac{1}{2} (Y - (f - \eta(f)))^2 - \frac{1}{2} (Y - f)^2 - \frac{1}{2} \eta(f)^2 \right] \right. \\
&\quad \left. - \frac{1}{n} \sum_i \left[\frac{1}{2} (Y_i - (f_i - \eta(f_i)))^2 - \frac{1}{2} (Y - f_i)^2 - \frac{1}{2} \eta(f_i)^2 \right] \right).
\end{aligned}$$

819 By setting

$$\begin{aligned}
\Phi(S) &= \sup_{f \in \mathcal{F}} \sup_{\eta} \mathbb{E} \left[\frac{1}{2} (Y - (f - \eta(f)))^2 - \frac{1}{2} (Y - f)^2 - \frac{1}{2} \eta(f)^2 \right] \\
&\quad - \frac{1}{n} \sum_i \left[\frac{1}{2} (Y_i - (f_i - \eta(f_i)))^2 - \frac{1}{2} (Y - f_i)^2 - \frac{1}{2} \eta(f_i)^2 \right],
\end{aligned}$$

820 From the proof of Theorem 3.3 in Mohri et al. [32], we have, with probability at least $1 - \delta$,

$$\Phi(S) \leq \mathbb{E}_S[\phi(S)] + \sqrt{\frac{\log \frac{1}{\delta}}{2n}}.$$

This can be shown using McDiarmid's inequality, following the same argument as in the proof of Theorem 3.3 in Mohri et al. [32] since

$$\eta(f(X)) \cdot (Y - f(X)) = \frac{1}{2} (Y_i - (f_i - \eta(f_i)))^2 - \frac{1}{2} (Y - f_i)^2 - \frac{1}{2} \eta(f_i)^2$$

821 and the constants for the bounded differences in McDiarmid's inequality are equal to 1, and thus the
822 result is identical to that appearing in Theorem 3.3 in Mohri et al. [32].

823 We then set $\omega(f, \eta, Y, X) = \frac{1}{2} (Y - (f - \eta(f)))^2 - \frac{1}{2} (Y - f)^2 - \frac{1}{2} \eta(f)^2$, and by the standard
824 symmetrization argument, we have

$$\mathbb{E}_S[\phi(S)] \leq 2 \mathbb{E}_{\sigma, S} \left[\sup_f \sup_{\eta} \frac{1}{n} \sum_{i=1}^n \sigma_i \omega(f, \eta, Y_i, X_i) \right].$$

825 Then by the property of the supremum,

$$\begin{aligned} & \mathbb{E}_{\sigma,S} \left[\sup_f \sup_{\eta} \frac{1}{n} \sum_{i=1}^n \sigma_i \omega(f, \eta, Y_i, X_i) \right] \\ & \leq \frac{1}{2} \mathbb{E}_{\sigma,S} \left[\sup_f \sup_{\eta} \frac{1}{n} \sum_{i=1}^n \sigma_i (Y_i - (f_i - \eta(f_i)))^2 \right] + \frac{1}{2} \mathbb{E}_{\sigma,S} \left[\sup_f \sup_{\eta} \frac{1}{n} \sum_{i=1}^n \sigma_i (Y_i - f_i)^2 \right] \\ & \quad + \frac{1}{2} \mathbb{E}_{\sigma,S} \left[\sup_f \sup_{\eta} \frac{1}{n} \sum_{i=1}^n \sigma_i \eta(f_i)^2 \right]. \end{aligned}$$

826 Then, from Propositions 11.2 and 11.2 in Mohri et al. [32],

$$\frac{1}{2} \mathbb{E}_{\sigma,S} \left[\sup_f \sup_{\eta} \frac{1}{n} \sum_{i=1}^n \sigma_i (Y_i - (f_i - \eta(f_i)))^2 \right] \leq \mathbb{E}_{\sigma,S} \left[\sup_f \sup_{\eta} \frac{1}{n} \sum_{i=1}^n \sigma_i (f_i - \eta(f_i)) \right] \leq \mathfrak{R}_{\mathcal{D},n}(\mathcal{F})$$

827 and

$$\frac{1}{2} \mathbb{E}_{\sigma,S} \left[\sup_f \sup_{\eta} \frac{1}{n} \sum_{i=1}^n \sigma_i (Y_i - f_i)^2 \right] \leq \mathbb{E}_{\sigma,S} \left[\sup_f \sup_{\eta} \frac{1}{n} \sum_{i=1}^n \sigma_i f_i \right] \leq \mathfrak{R}_{\mathcal{D},n}(\mathcal{F})$$

828 and

$$\frac{1}{2} \mathbb{E}_{\sigma,S} \left[\sup_f \sup_{\eta} \frac{1}{n} \sum_{i=1}^n \sigma_i \eta(f_i)^2 \right] \leq \mathbb{E}_{\sigma,S} \left[\sup_f \sup_{\eta} \frac{1}{n} \sum_{i=1}^n \sigma_i \eta(f_i) \right] \leq \mathfrak{R}_{\mathcal{D},n}(\mathcal{F})$$

829 holds. In conclusion, we have

$$\mathbb{E}_S[\phi(S)] \leq 6\mathfrak{R}_{\mathcal{D},n}(\mathcal{F})$$

830 where we used the composition assumption that $f + \eta \circ f \in \mathcal{F}$ in the last inequality. This concludes
831 the proof. \square

832 A.3 Proof of Theorem 5

833 *Proof.* From Proposition 7 in Rakhlin and Zhai [35], the RKHS associated with the Laplace kernel
834 on \mathbb{R} corresponds to the Sobolev space $H^1 = W^{2,1}$ (see also Buchholz [7]). Then, by Theorem
835 6 in Bourdaud [5], the composition of a Lipschitz function with a function in H^1 remains in
836 H^1 . To apply Theorem 6, the Lipschitz function r must satisfy $r(0) = 0$. If $r(0) \neq 0$, define
837 $\tilde{r}(x) = r(x) - r(0)$, so that $\tilde{r} \circ f \in H^1$. Since constant functions are included in the Sobolev space,
838 we have $r \circ f(x) = \tilde{r} \circ f(x) + r(0) \in H^1$.

839 Similarly, Theorem 7 in Bourdaud [5] shows that the composition of $k \in H^1$ and $f \in H^1$ yields
840 $k \circ f \in H^1$. \square

841 A.4 Proof of Corollary 2

842 *Proof.* The corresponding Rademacher complexity is

$$\begin{aligned} \hat{\mathfrak{R}}_S(\mathcal{F}) &= \frac{1}{n} \mathbb{E}_{\sigma} \left[\sup_{(f,b) \in \mathcal{F}} \sum_{i=1}^n \sigma_i (f(x_i) + b) \right] \\ &= \frac{1}{n} \mathbb{E}_{\sigma} \left[\sup_{\|f\|_{\mathcal{H}} \leq \alpha, |b| \leq \alpha \Lambda + 1} \sum_{i=1}^n \sigma_i f(x_i) + \sum_{i=1}^n \sigma_i b \right] \\ &\leq \frac{1}{n} \mathbb{E}_{\sigma} \left[\sup_{\|f\|_{\mathcal{H}} \leq \alpha} \sum_{i=1}^n \sigma_i f(x_i) \right] + \frac{1}{n} \mathbb{E}_{\sigma} \left[\sup_{|b| \leq \alpha \Lambda + 1} \sum_{i=1}^n \sigma_i b \right] \end{aligned}$$

843 The first term can be bounded by $\alpha \Lambda / \sqrt{n}$ from the standard derivation of the Rademacher complexity
844 for the kernel functions, see Mohri et al. [32] for the derivation. The second term is that the

845 supremeum with respect to b is that if $\sum \sigma_i$ is positive, then $b = \alpha\Lambda + 1$, if $\sum \sigma_i$ is negative, then
846 $b = -(\alpha\Lambda + 1)$.

847 Thus, from the Massart's lemma, where the hypothesis set is

$$\{(\alpha\Lambda + 1), -(\alpha\Lambda + 1)\} \subset \mathbb{R}^1$$

848 Thus, by setting $A := \{(\Lambda + 1), -(\Lambda + 1)\} \subset \mathbb{R}$ and this results in

$$\frac{1}{n} \mathbb{E}_\sigma \left[\sup_{|b| \leq \Lambda + 1} \sum_{i=1}^n \sigma_i b \right] = \frac{1}{n} \mathbb{E}_\sigma \left[\sup_{z \in A} \sum_{i=1}^n \sigma_i z_i \right] \leq \frac{\sqrt{2 \log 2} (\Lambda + 1)}{\sqrt{n}} \leq \frac{2(\Lambda + 1)}{\sqrt{n}}$$

849 In conclusion, we have

$$\hat{\mathfrak{R}}_S(\mathcal{F}) \leq \frac{3\Lambda + 2}{\sqrt{n}}.$$

850 We obtain the result. \square

851 A.5 Proof of Theorem 6

852 *Proof.* From Proposition 7 in Rakhlin and Zhai [35], the RKHS associated with the Laplace kernel
853 on \mathbb{R}^d is the Sobolev space $H^s = W^{2,s}$ with $s = (d+1)/2$ (see also Buchholz [7]). According to
854 Theorem 7 in Bourdaud [5], for given functions f and r , we have $r \circ f \in H^s$ if and only if $r \in H^s$.
855 However, here we take r from a Lipschitz function class, so r is not generally in H^s , and thus the
856 result follows.

857 Similarly, $k \in \mathcal{K}_1$ implies $k \in H^1$ but not $k \in H^s$. Therefore, we obtain the result. \square

858 A.6 Proof of Theorem 7

859 *Proof.* We use the approximation theory given in Corollary 5.29 of Steinwart and Christmann [36],
860 which states that for a continuous Nemitski loss function ℓ , the Bayes risk and the minimum achievable
861 risk within the RKHS are equivalent. According to Definition 2.16 in Steinwart and Christmann [36],
862 the squared loss with L_2 regularization is a Nemitski loss function. Then, Corollary 5.29 implies that

$$\inf_f L(f) = \inf_{f \in \mathcal{F}} L(f),$$

863 where the infimum on the left-hand side is taken over all measurable functions from $\mathcal{X} \rightarrow \mathbb{R}$. This
864 equivalence follows from the approximation power of universal kernels; see the proof of Corollary
865 5.29 in Steinwart and Christmann [36] for details.

866 With this in mind, and following the argument in the proof of Claim 5.1 in Błasiok et al. [3], we
867 upper bound the post-processing gap as follows. By the definition of the infimum,

$$f^* = \operatorname{argmin}_{f \in \mathcal{F}} \mathbb{E} \ell_{\text{sq}}(f(X), Y) + \lambda \|f\|_{\mathcal{F}}^2.$$

868 Consider the solution f^* and an arbitrary $h \in \text{Lip}_{L=1}$. Note that $f^* + h \circ f^*$ is a measurable function.
869 For notational simplicity, we denote $r \circ f^* := f^* + h \circ f^*$.

$$\begin{aligned} & \mathbb{E} \ell_{\text{sq}}(f_n^*(X), Y) - \mathbb{E} \ell_{\text{sq}}(r \circ f_n^*(X), Y) \\ &= \mathbb{E} \ell_{\text{sq}}(f_n^*(X), Y) + \lambda \|f\|_{\mathcal{F}}^2 - \lambda \|f\|_{\mathcal{F}}^2 - \mathbb{E} \ell_{\text{sq}}(r \circ f_n^*(X), Y) \\ &\leq L(f_n^*) - L(f^*) + L(f^*) - L(r \circ f_n^*) + 2\lambda \\ &\leq L(f^*) + \text{err}_{\text{ex}}(n) - L(r \circ f_n^*) + 2\lambda \\ &\leq 2\lambda + \text{err}_{\text{ex}}(n) \end{aligned}$$

870 In the last inequality, we used the fact that

$$L(f^*) - L(r \circ f_n^*) = \inf_{f \in \mathcal{F}} L(f) - L(r \circ f_n^*) = \inf_f L(f) - L(r \circ f_n^*) \leq 0$$

871 Since infimum is taken with respect to all measurable functions, therefore $\inf_f L(f) \leq L(r \circ f_n^*)$
872 holds.

873 Next we upper bound $\text{err}_{\text{ex}}(n)$. This is well studied in the literature of the generalization analysis
874 and from Proposition 4.1 in Mohri et al. [32], we have

$$L(f_n^*) - \inf_{f \in \mathcal{F}} L(f) \leq \text{err}_{\text{ex}}(n) \leq 2 \sup_{f \in \mathcal{F}} |L(f) - L_n(f)| \leq 2 \left(2\mathfrak{R}_{\mathcal{D},n}(\mathcal{F}) + \sqrt{\frac{\log \frac{2}{\delta}}{2n}} \right).$$

875 Then we have

$$\text{smCE}(f_n^*, \mathcal{D}) \leq \sqrt{2\lambda + 4\mathfrak{R}_{\mathcal{D},n}(\mathcal{F}) + \sqrt{2\frac{\log \frac{2}{\delta}}{n}}}.$$

876 \square

877 A.7 Proof of Corollary 3

878 We first upper bound the training dual smooth CE. The proof is almost identical to that of Theorem 3.
879 We first introduce the training dual smooth CE as

$$\text{smCE}^{(\psi,1/4)}(g, S) := \sup_{h \in \text{Lip}_{1/4}(\mathbb{R}, [-1,1])} \frac{1}{n} \sum_{i=1}^n [h(g(X_i)) \cdot (Y_i - f(X_i))].$$

880 We also define the empirical counterpart of the dual post-processing gap as

$$\text{pGap}^{(\psi,1/4)}(g, S) := \frac{1}{n} \sum_{i=1}^n \ell^\psi(g(X_i), Y_i) - \inf_{h \in \text{Lip}_{L=1}(\mathbb{R}, [-4,4])} \frac{1}{n} \sum_{i=1}^n \ell^\psi(f(X_i) + h(g(X_i)), Y_i)$$

881 We can prove that

$$2\text{smCE}^{(\psi,1/4)}(g, S)^2 \leq \text{pGap}^{(\psi,1/4)}(g, S) \leq 4\text{smCE}^{(\psi,1/4)}(g, S). \quad (4)$$

882 The proof of this is exactly the same as that of Lemma 4.7 in Błasiok et al. [3], where we simply
883 replace the expectation by \mathcal{D} with that of the empirical expectation.

884 To simplify the notation, we express $r \circ g := g + h \circ g$. Then we will upper bound the training

$$\begin{aligned} & \frac{1}{n} \sum_{i=1}^n \ell^\psi(g(X_i), Y_i) - \inf_{h \in \text{Lip}_{L=1}(\mathbb{R}, [-4,4])} \frac{1}{n} \sum_{i=1}^n \ell^\psi(r \circ g(X_i), Y_i) \\ &= \frac{1}{n} \sum_{i=1}^n \ell^\psi(g(X_i), Y_i) + \lambda \|g\|_{\mathcal{G}}^2 - \lambda \|g\|_{\mathcal{G}}^2 - \inf_{h \in \text{Lip}_{L=1}(\mathbb{R}, [-4,4])} \frac{1}{n} \sum_{i=1}^n \ell^\psi(r \circ g(X_i), Y_i) \\ &= \frac{1}{n} \sum_{i=1}^n \ell^\psi(g(X_i), Y_i) + \lambda \|g\|_{\mathcal{G}}^2 - \lambda \|g\|_{\mathcal{G}}^2 \\ &\quad - \inf_{h \in \text{Lip}_{L=1}(\mathbb{R}, [-4,4])} \left(\frac{1}{n} \sum_{i=1}^n \ell^\psi(r \circ g(X_i), Y_i) + \lambda \|r \circ g\|_{\mathcal{G}}^2 - \lambda \|r \circ g\|_{\mathcal{G}}^2 \right) \\ &= L_n(g) - \inf_{h \in \text{Lip}_{L=1}(\mathbb{R}, [-4,4])} \left(\frac{1}{n} \sum_{i=1}^n \ell^\psi(r \circ g(X_i), Y_i) + \lambda \|r \circ g\|_{\mathcal{G}}^2 + \lambda \|g\|_{\mathcal{G}}^2 - \lambda \|r \circ g\|_{\mathcal{G}}^2 \right) \\ &\leq L_n(g) - \inf_{h \in \text{Lip}_{L=1}(\mathbb{R}, [-4,4])} \left(\frac{1}{n} \sum_{i=1}^n \ell^\psi(r \circ g(X_i), Y_i) + \lambda \|r \circ g\|_{\mathcal{G}}^2 \right) \\ &\quad - \inf_{h \in \text{Lip}_{L=1}(\mathbb{R}, [-4,4])} (\lambda \|g\|_{\mathcal{G}}^2 - \lambda \|r \circ g\|_{\mathcal{G}}^2) \\ &\leq L_n(g_n^*) + \text{err}_n(g) - \inf_{h \in \text{Lip}_{L=1}(\mathbb{R}, [-4,4])} \left(\frac{1}{n} \sum_{i=1}^n \ell^\psi(r \circ g(X_i), Y_i) + \lambda \|r \circ g\|_{\mathcal{G}}^2 \right) + 2\lambda G^2 \\ &= L_n(g_n^*) + \text{err}_n(g) - \inf_{h \in \text{Lip}_{L=1}(\mathbb{R}, [-4,4])} L_n(r \circ g) + 2\lambda G^2 \\ &\leq \text{err}_n(g) + 2\lambda G^2 \end{aligned}$$

885 where we used that $L_n(f) = L_n(f_n^*) + \text{err}_n(f)$ and

$$\|r \circ g\|_{\mathcal{G}}^2 - \|g\|_{\mathcal{G}}^2 = (\|r \circ g\|_{\mathcal{G}} + \|g\|_{\mathcal{G}})(\|r \circ g\|_{\mathcal{G}} - \|g\|_{\mathcal{G}}) \leq 2\|r \circ g - g\|_{\mathcal{G}} \leq 2G^2$$

886 Moreover, we used the relation

$$L_n(g_n^*) \leq \inf_{h \in \text{Lip}_{L=1}(\mathbb{R}, [-4, 4])} L_n(r \circ g)$$

887 in the last line. Then using Eq. (4), we have the upper-bound for the training dual smooth CE.

888 Next, we study the generalization error for $\text{smCE}^{(\psi, 1/4)}(g, \mathcal{D})$

$$\begin{aligned} & \text{smCE}^{(\psi, 1/4)}(g, \mathcal{D}) - \text{smCE}^{(\psi, 1/4)}(g, S) \\ &= \sup_h \mathbb{E} h(g(X)) \cdot (Y - f(X)) - \sup_{h'} \frac{1}{n} \sum_i h'(g(X_i)) \cdot (Y_i - f(X_i)) \\ &= \sup_h \mathbb{E} \left[\frac{1}{2}(Y - (f - h(g(X)))^2 - \frac{1}{2}(Y - f)^2 - \frac{1}{2}h(g(X))^2 \right] \\ &\quad - \sup_{h'} \frac{1}{n} \sum_i \left[\frac{1}{2}(Y_i - (f_i - h'(g(X_i)))^2 - \frac{1}{2}(Y_i - f_i)^2 - \frac{1}{2}h'(g(X_i))^2 \right] \\ &\leq \sup_{\eta} \left(\mathbb{E} \left[\frac{1}{2}(Y - (f - h(g(X)))^2 - \frac{1}{2}(Y - f)^2 - \frac{1}{2}h(g(X))^2 \right] \right. \\ &\quad \left. - \frac{1}{n} \sum_i \left[\frac{1}{2}(Y_i - (f_i - h(g(X_i)))^2 - \frac{1}{2}(Y_i - f_i)^2 - \frac{1}{2}h(g(X_i))^2 \right] \right) \end{aligned}$$

889 Then we proceed the proof exactly in the same way as Appendix A.2.

890 A.8 Proof of Corollary 4

891 By the assumptions, we can apply Corollary 3 to this setting. All we need is to estimate the
892 Rademacher complexity.

893 We then define the set of functions obtained by $\sigma(g)$ for any $g \in \mathcal{G}$ as \mathcal{F} , and σ is 1/4 Lipschitz
894 function,

$$\hat{\mathfrak{R}}_S(\mathcal{F}) \leq \frac{1}{4}\hat{\mathfrak{R}}_S(\mathcal{G})$$

895 and $\hat{\mathfrak{R}}_S(\mathcal{G})$ can be bounded exactly in the same way as the proof of Corollary 2.

896 Here we also present the result that corresponds to Theorem 7:

897 **Theorem 8.** Let k be a universal kernel with associated RKHS \mathcal{H} . Let $\mathcal{G} = \mathcal{H} \oplus \mathbb{R} = \{g + b \mid g \in$
898 $\mathcal{H}, b \in \mathbb{R}\}$. Suppose there exist constants Λ and α such that $\sup_{x, x' \in \mathcal{X}} k(x, x') \leq \Lambda$, $\|g\|_{\mathcal{H}} \leq \alpha$,
899 and $|b| \leq \alpha\Lambda + 1$. Then, with probability at least $1 - \delta$ over the draw of the training dataset, it holds
900 that

$$\text{smCE}^{(\psi, 1/4)}(g_n^*, \mathcal{D}) \leq \sqrt{2\lambda G^2 + \frac{3\alpha\Lambda + 2}{\sqrt{n}} + \sqrt{\frac{2 \log \frac{2}{\delta}}{n}}}.$$

901 The proof of this theorem is almost identical to that of Theorem 7, since the logistic loss is also a
902 continuous Nemitski loss and thus, we can apply the same techniques.

903 B Additional discussion

904 B.1 Post processing gap and Calibration metrics

905 Following Błasior et al. [3], we introduce the general proper loss function and its relation to the
906 post-processing gap.

907 A proper loss function ℓ can always be represented using a convex function ϕ as follows:

$$\ell(p, y) = -\phi(p) - \nabla\phi(p) \cdot (y - p),$$

908 where $\phi : [0, 1] \rightarrow \mathbb{R}$ is a convex function and $\nabla\phi(p)$ denotes a subgradient at p . Following Błasik et al. [3], we assume that ϕ is differentiable.

910 We define the convex conjugate of the function $\phi(p)$ as follows: for all $s \in \mathbb{R}$,

$$\psi(s) = \sup_{p \in [0, 1]} \{s \cdot p - \phi(p)\}.$$

911 The *dual loss* $\ell^\psi : \mathbb{R} \times \mathcal{Y} \rightarrow \mathbb{R}$ is then defined as

$$\ell^\psi(s, y) := \psi(s) - s \cdot y.$$

912 By Fenchel–Young duality, this relationship is inverted as $p = \nabla\psi(s)$, and with these definitions, the
913 proper loss can equivalently be written as

$$\ell(p, y) = \ell^\psi(\nabla\phi(p), y) = \psi(\nabla\phi(p)) - \nabla\phi(p) \cdot y.$$

914 We remark that the relation $p = \nabla\psi(s)$ can be interpreted as mapping logits to predicted probabilities.
915 For details and proofs, see Błasik et al. [3].

916 Błasik et al. [3] considered modeling the score function s by a function g , and then applying the
917 transformation $p = \nabla\psi(s)$. Thus, they proposed to apply post-processing to g , which leads to the
918 following definition:

919 **Definition 5** (Dual post-processing gap). *Assume that ψ is a differentiable and convex function with
920 derivative $\nabla\psi(t) \in [0, 1]$ for all $t \in \mathbb{R}$, and that ψ is λ -smooth. Given ψ , ℓ^ψ , $g : \mathcal{X} \rightarrow \mathbb{R}$, and
921 distribution \mathcal{D} , we define the dual post-processing gap as*

$$\text{pGap}^{(\psi, \lambda)}(g, \mathcal{D}) := \mathbb{E}[\ell^\psi(g(X), Y)] - \inf_{h \in \text{Lip}_1(\mathbb{R}, [-1/\lambda, 1/\lambda])} \mathbb{E}[\ell^\psi(g(X) + h(g(X)), Y)].$$

922 When considering the cross-entropy loss, the dual post-processing gap corresponds to improving the
923 logit function.

924 **Definition 6** (Dual smooth calibration). *Consider the same setting as in the definition of the dual
925 post-processing gap. Given ψ and g , define $f(\cdot) = \nabla\psi(g(\cdot))$. The dual calibration error of g is
926 defined as*

$$\text{smCE}^{(\psi, \lambda)}(g, \mathcal{D}) := \sup_{h \in \text{Lip}_{L=\lambda}(\mathbb{R}, [-1, 1])} \mathbb{E}[\eta(g(X)) \cdot (Y - f(X))].$$

927 Then, similarly to the relationship between the smooth ECE and the post-processing gap, the following
928 holds: if ψ is a λ -smooth function, then

$$\frac{1}{2} \text{smCE}^{(\psi, \lambda)}(g, \mathcal{D})^2 \leq \frac{\lambda}{2} \text{pGap}^{(\psi, \lambda)}(g, \mathcal{D})^2 \leq \text{smCE}^{(\psi, \lambda)}(g, \mathcal{D}),$$

929 and

$$\text{smCE}(f, \mathcal{D}) \leq \text{smCE}^{(\psi, \lambda)}(g, \mathcal{D})$$

930 also holds. Thus, by studying the dual post-processing gap, we can obtain bounds on the smooth
931 calibration error. By considering L_2 -regularized objective function $\mathbb{E}[\ell^\psi(g(X), Y)] + \|g\|_{\mathcal{G}}^2$ and its
932 empirical counterpart, we can develop the theory for the general dual smooth CE and ERM in a
933 similar way to the case of the squared and cross-entropy loss.

934 B.2 Relationships different calibration metrics

935 Błasik et al. [2] introduced the ground truth distance for calibration, defined as follows:

936 **Definition 7** (True distance to calibration). *We define the true distance of a predictor f from
937 calibration as*

$$\text{dCE}_{\mathcal{D}}(f) := \inf_{g \in \text{cal}(\mathcal{D})} \mathbb{E}_{\mathcal{D}} |f(x) - g(x)|,$$

938 where $\text{cal}(\mathcal{D})$ denotes the set of predictors that are perfectly calibrated with respect to \mathcal{D} .

939 This provides an ideal notion for measuring calibration; see Błasik et al. [2] for details. They showed
940 that the smooth CE both upper and lower bounds the true distance to calibration:

$$\text{smCE}(f, \mathcal{D}) \leq \text{dCE}_{\mathcal{D}}(f) \leq 4\sqrt{2\text{smCE}(f, \mathcal{D})}.$$

941 On the other hand, the commonly used ECE, defined as

$$\text{ECE}_{\mathcal{D}}(f) := \mathbb{E}_{\mathcal{D}} [\|\mathbb{E}_{\mathcal{D}}[y|f(x)] - f(x)\|],$$

942 is discontinuous, and Błasik et al. [2] showed that ECE does not lower bound $\text{dCE}_{\mathcal{D}}(f)$ unless
943 continuity of the conditional expectation is assumed.

944 Błasik et al. [2] also established the relationship between $\text{dCE}_{\mathcal{D}}(f)$ and the binned ECE. Given a
945 partition $\mathcal{I} = \{I_1, \dots, I_m\}$ of $[0, 1]$ into intervals, the binned ECE is defined as

$$\text{binnedECE}_{\mathcal{D}}(f, \mathcal{I}) = \sum_{j \in [m]} |\mathbb{E}[(f - y)\mathbb{1}(f \in I_j)]|.$$

946 They showed that by adding the bin widths and minimizing over the choice of partition, we obtain
947 the following definition:

$$\text{intCE}(f) := \min_{\mathcal{I}} (\text{binnedECE}_{\mathcal{D}}(f, \mathcal{I}) + w(\mathcal{I})),$$

948 where

$$w(\mathcal{I}) := \sum_{j \in [m]} |\mathbb{E}w(I_j)\mathbb{1}(f \in I_j)|,$$

949 and $w(I)$ denotes the width of interval I . Then, the following bound holds (Theorem 6.3 in Błasik
950 et al. [2]):

$$\text{dCE}_{\mathcal{D}}(f) \leq \text{intCE}(f) \leq 4\sqrt{\text{dCE}_{\mathcal{D}}(f)}.$$

951 As we have seen, bounding the smooth CE leads to a bound on $\text{dCE}_{\mathcal{D}}(f)$, which in turn bounds
952 $\text{intCE}(f)$, which corresponds to the binned ECE, which is optimized with respect to the partition.

953 C Details of experimental settings

954 In this section, we summarize the detail information of our numerical experiments in Section 5. Our
955 experiments were conducted on NVIDIA GPUs with 32GB memory (NVIDIA DGX-1 with Tesla
956 V100 and DGX-2).

Table 2: Datasets used in our experiments

Dataset	Classes	Train data (n_{tr})	Recalibration data (n_{re})	Test data (n_{te})
KITTI	2	16000	1000	8000
PCam	2	22768	1000	9000

957 C.1 Toy data experiments ($\mathcal{X} = \mathbb{R}$)

958 To investigate the behavior of different kernel-based methods under controlled conditions, we first
959 conduct experiments on synthetic two-dimensional binary classification tasks. These toy experiments
960 serve to isolate and visualize model behavior with respect to classification performance and calibration
961 quality, without the confounding factors present in real-world datasets.

962 **Data generation.** We generate synthetic data using a simple but structured stochastic process.
963 For each of n samples, a binary label $y \in \{0, 1\}$ is drawn independently from a Bernoulli(0.5)
964 distribution. Given the label, the input feature $x \in \mathbb{R}^2$ is sampled from a Gaussian distribution
965 centered at $\mu_1 = [-1, -1]^T$ for $y = 1$, and at $\mu_0 = [1, 1]^T$ for $y = 0$, with identity covariance
966 $\Sigma = I_2$ in both cases. That is,

$$x | y = 1 \sim \mathcal{N}([-1, -1]^T, I), \quad x | y = 0 \sim \mathcal{N}([1, 1]^T, I).$$

967 This construction induces a smooth but nonlinear Bayes decision boundary, suitable for evaluating
968 kernel methods.

969 **Models and kernels.** We evaluate two models:

- 970 • **KRR**: Kernel Ridge Regression with theoretically motivated $\lambda_n = n^{-1/2}$ for Gaussian
971 kernels and $\lambda_n = n^{-1/3}$ for Laplace kernels.
972 • **KLR**: Kernel Logistic Regression optimized via gradient descent.

973 Each model is evaluated using two kernels: the Gaussian kernel $k(x, x') = \exp(-\|x - x'\|^2/2\sigma^2)$
974 and the Laplace kernel $k(x, x') = \exp(-\|x - x'\|/\sigma)$. For each kernel, the bandwidth σ is selected
975 using the median heuristic on the training data.

976 **Metrics.** We assess both accuracy and calibration using the following metrics:

- 977 • **Kernel Calibration Error (KCE)**: Evaluated with both Gaussian and Laplace kernels, with
978 σ determined by a heuristic on the predicted confidence vector.
979 • **Smooth Calibration Error (SCE)**: A continuous variant of calibration error designed for
980 better sample efficiency.
981 • **Expected Calibration Error (ECE)**: Classical binning-based calibration metric with the
982 number of bins set to $\lfloor n^{1/3} \rfloor$ for n data points, following Futami and Fujisawa [13], Fujisawa
983 and Futami [12].

984 **Experimental protocol.** We evaluate performance as a function of training set size, with n_{train}
985 logarithmically spaced from 100 to 10,000. For each setting, experiments are repeated with 10
986 different random seeds for robustness. We also evaluate sensitivity to the regularization parameter λ
987 by fixing $n_{\text{train}} = 10,000$ and varying λ over a logarithmic grid from 10^{-4} to 10^2 .

988 **Implementation.** All methods are implemented using PyTorch. Gradient descent for KLR is run
989 for up to 1,000 iterations with a step size of 0.01 and stopping tolerance of 10^{-6} . Results are reported
990 on both training and test sets. Each experiment logs the metrics above and saves results in a CSV
991 format for post-hoc statistical analysis.

992 **C.2 Recalibration experiments ($\mathcal{X} = \mathbb{R}$)**

993 We provide the details of the datasets along with the number of training, recalibration, and test
994 samples in Table 2. For the models, we used XGBoost [8], Random Forests [6], and a one-layer
995 neural network (NN) for the KITTI and PCam experiments. All experiments—including the training
996 of XGBoost, Random Forests, and the one-layer NN—were conducted using code adapted from
997 Wenger et al. [39]¹.

998 **Performance evaluation:** We evaluated predictive accuracy and binned ECE, using $B = \lfloor n_{\text{re}}^{1/3} \rfloor$,
999 in accordance with the theoretical insights from Futami and Fujisawa [13], Fujisawa and Futami [12].
1000 Additionally, we included two other calibration metrics: KCE and SCE. To train the recalibration
1001 functions, we performed 10-fold cross-validation and reported the mean and standard deviation of
1002 both performance metrics.

1003 **C.3 Real dataset experiments (Binary classification benchmarks; $\mathcal{X} = \mathbb{R}^d$)**

1004 We perform binary classification experiments using real-world tabular datasets to evaluate calibration
1005 and generalization performance across various kernel methods and sample sizes. Two separate
1006 protocols are employed:

1007 **(A) Sample size variation experiment.** This setting aims to evaluate how calibration performance
1008 evolves with increasing sample size. We consider the following methods: (i) KRR and (ii) KLR, each
1009 with either an RBF or Laplace kernel. For scalability, we use random Fourier features (RFF) for KLR.
1010 The Laplace kernel is approximated via a variant of RFF using samples from a Cauchy distribution.
1011 The corresponding feature mapping is implemented in our `LaplaceSampler` class.

¹<https://github.com/JonathanWenger/pycalib>

1012 For each dataset, we split the data into train/test with an 80/20 ratio while maintaining class balance.
1013 For training, we apply stratified subsampling of size $n \in \{50, \dots, 2000\}$ (log-spaced, with
1014 10 candidates). Each experiment is repeated with 5 different random seeds. The regularization
1015 hyperparameters are fixed as follows: $\alpha = 0.1$ for KLR and $\alpha = n^{-1/2}$ (RBF) or $\alpha = n^{-1/3}$
1016 (Laplace) for KRR, based on empirical performance.

1017 Bandwidth parameters for both kernels are selected via the median heuristic: for the RBF kernel,
1018 $\gamma = \frac{1}{2\sigma^2}$; for the Laplace kernel, $\gamma = \frac{1}{\sigma}$, where σ is the median pairwise Euclidean distance among
1019 training samples.

1020 **(B) Regularization parameter variation.** To assess sensitivity to the regularization hyperparameter,
1021 we fix the training set size at $n = 2000$ and vary α over a logarithmic grid: $\alpha \in \{10^{-4}, \dots, 10^2\}$.
1022 The same model families are considered as in (A), using fixed kernel parameters ($\gamma = 0.1$ for all
1023 models) to isolate the impact of α .

1024 **Evaluation metrics.** We report three calibration metrics: ECE with optimal bins [13, 12], smoothed
1025 ECE, and MMCE. For KRR, probabilities are obtained by clipping regression outputs to $[10^{-6}, 1 -$
1026 $10^{-6}]$ for stability.

1027 **Datasets.** We use six binary classification datasets from OpenML: kr-vs-kp, spambase, sick,
1028 churn, and Satellite. Features are standardized after applying appropriate imputation and one-
1029 hot encoding using scikit-learn pipelines. All preprocessing steps are fit only on the training set to
1030 avoid data leakage.

1031 **Reproducibility.** All experiments are implemented in Python using scikit-learn and CVXPY.
1032 Stratified sampling ensures class balance in subsamples. The full experimental code and data
1033 generation scripts will be made available upon publication.

1034 D Additional experimental results

1035 In this section, we present additional experimental results. Figures 3–5 show the complete results of
1036 our recalibration experiments described in Section 5.2. Consistent with our theoretical analysis, we
1037 observe that increasing the regularization parameter λ leads to higher smooth CE for both Laplace
1038 and Gaussian kernels, reflecting the expected effect of stronger regularization. Conversely, increasing
1039 the recalibration sample size n_{re} consistently lowers the smooth CE, demonstrating the anticipated
1040 convergence behavior. These findings highlight the practical applicability of our theory to real-world
1041 recalibration scenarios.

1042 We further show our experimental results on some real-world datasets explained in Appendix C.3
1043 in Figures 7 and 8. Similarly, we observe that setting the regularization parameter λ too small or
1044 too large results in unstable smooth CE values for both Laplace and Gaussian kernels. In contrast,
1045 increasing the recalibration sample size n_{re} consistently reduces the smooth CE in most cases,
1046 exhibiting convergence behavior aligned with our theoretical results. These findings further support
1047 the reliability of our theory, demonstrating its applicability to real-world binary classification tasks.

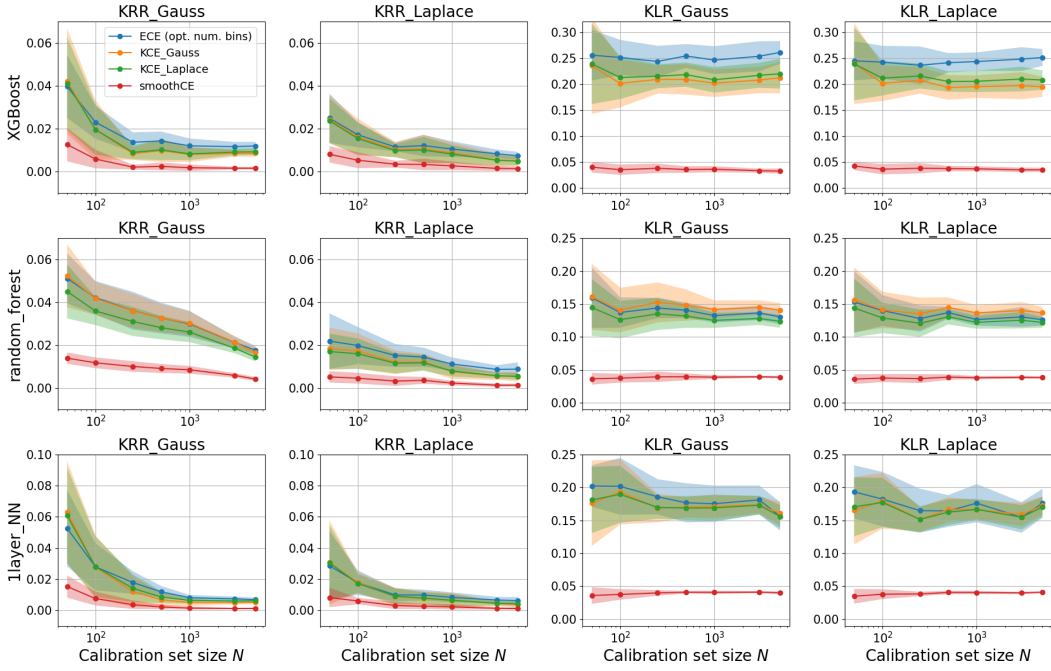


Figure 3: All Experimental Results of Recalibration: Effect of Recalibration Sample Size on Calibration Metrics on the KITTI dataset.

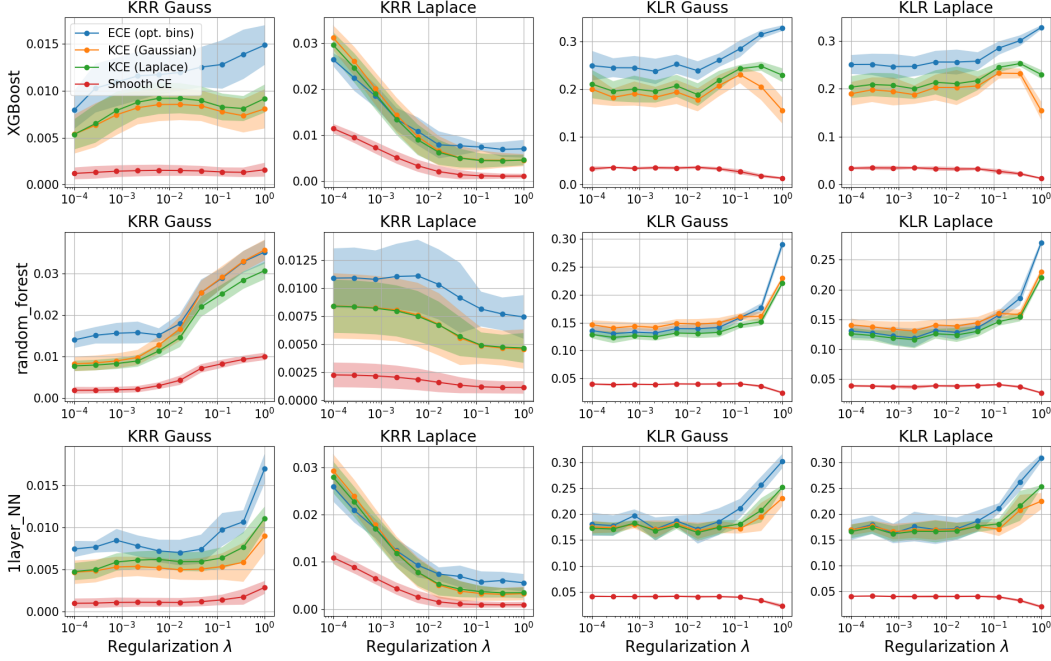


Figure 4: All Experimental Results of Recalibration: Effect of Regularization parameter λ on Calibration Metrics on the KITTI dataset.

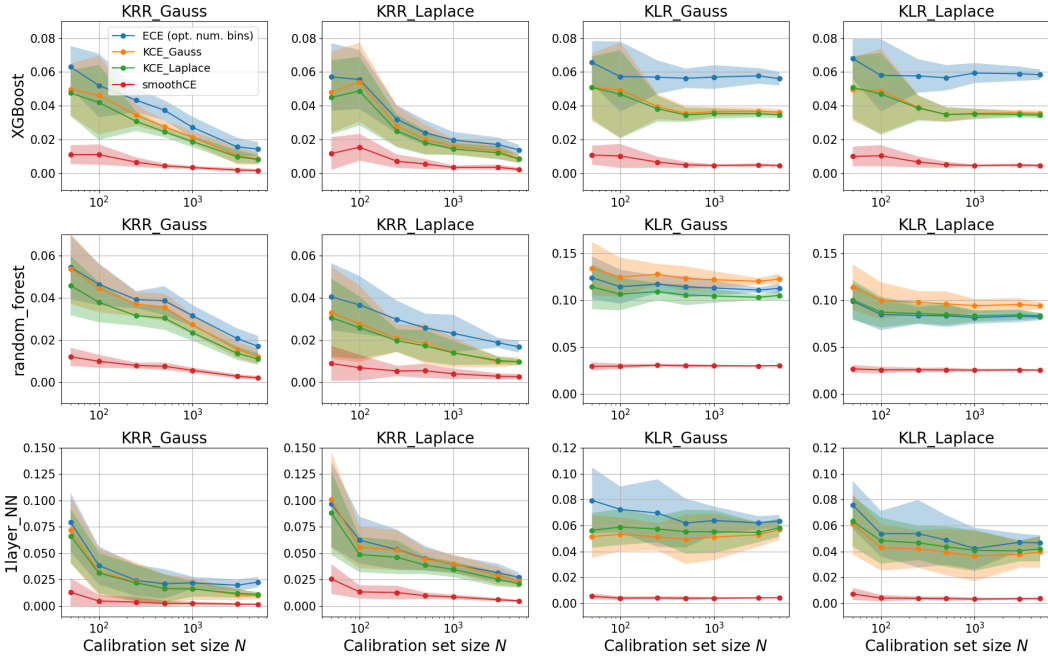


Figure 5: All Experimental Results of Recalibration: Effect of Recalibration Sample Size on Calibration Metrics on the PCam dataset.

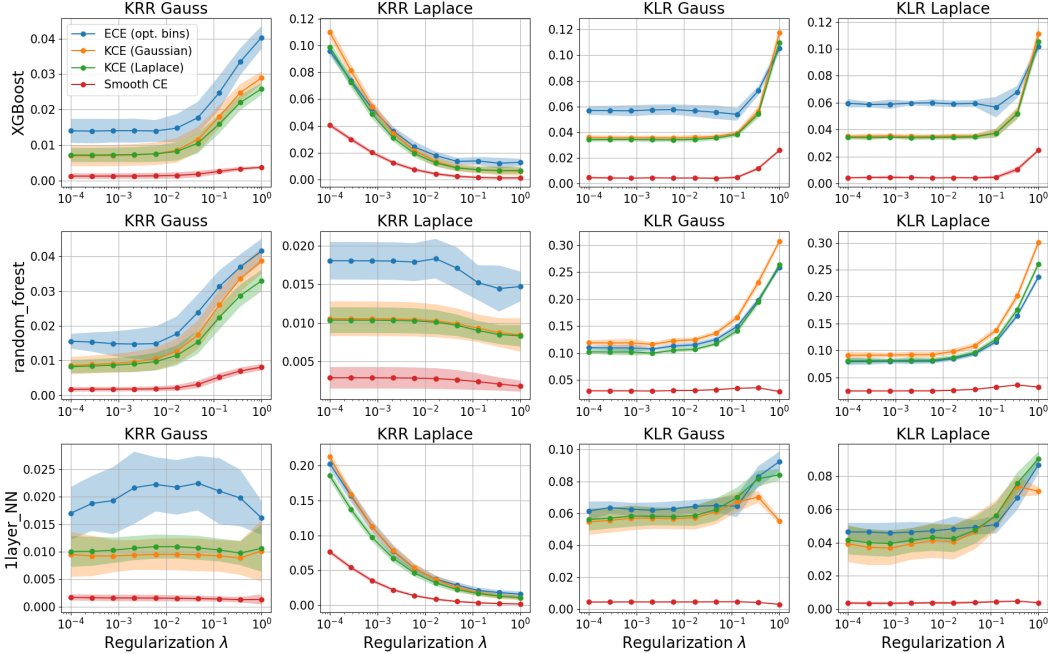


Figure 6: All Experimental Results of Recalibration: Effect of Regularization parameter λ on Calibration Metrics on the PCam dataset.

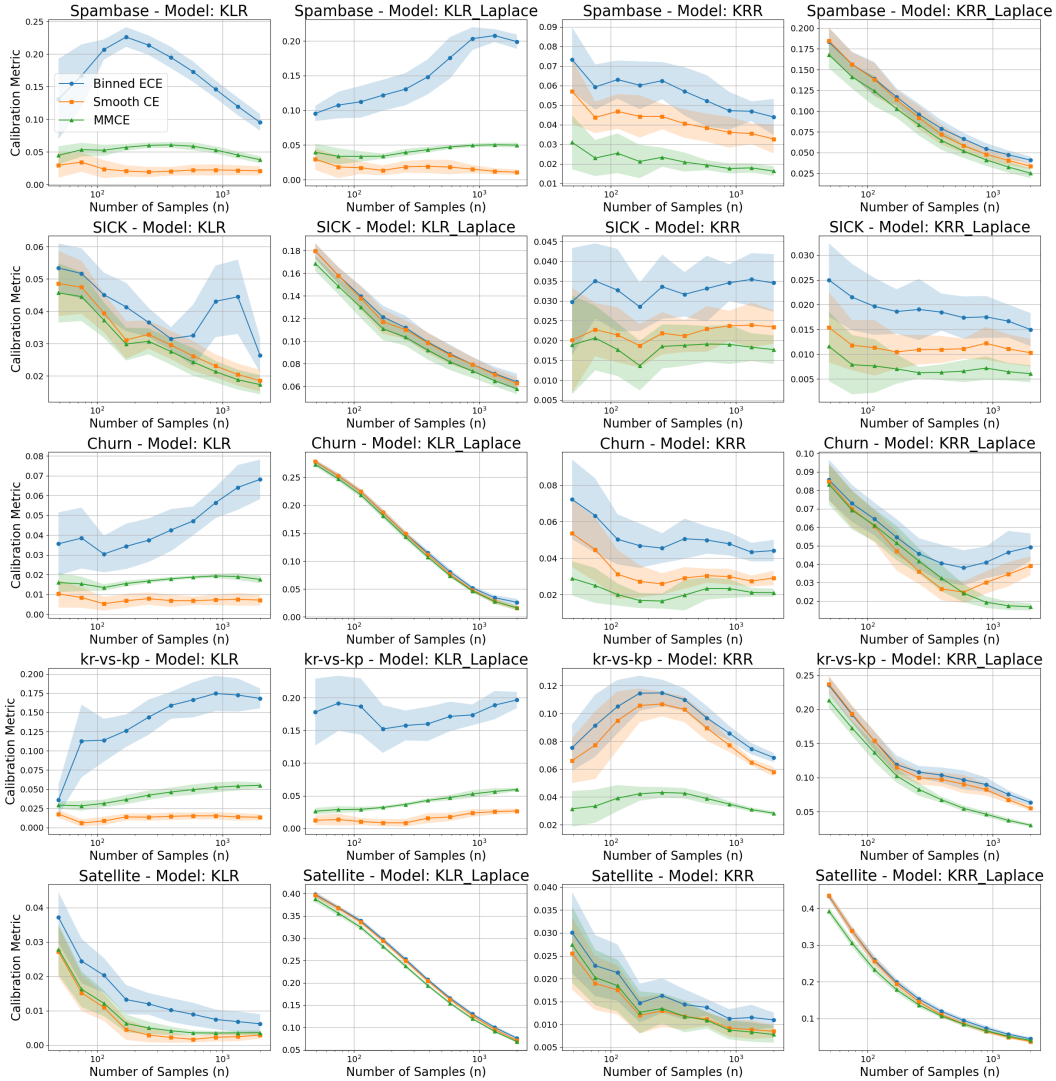


Figure 7: Effect of Sample Size on Calibration Metrics on the real world datasets.

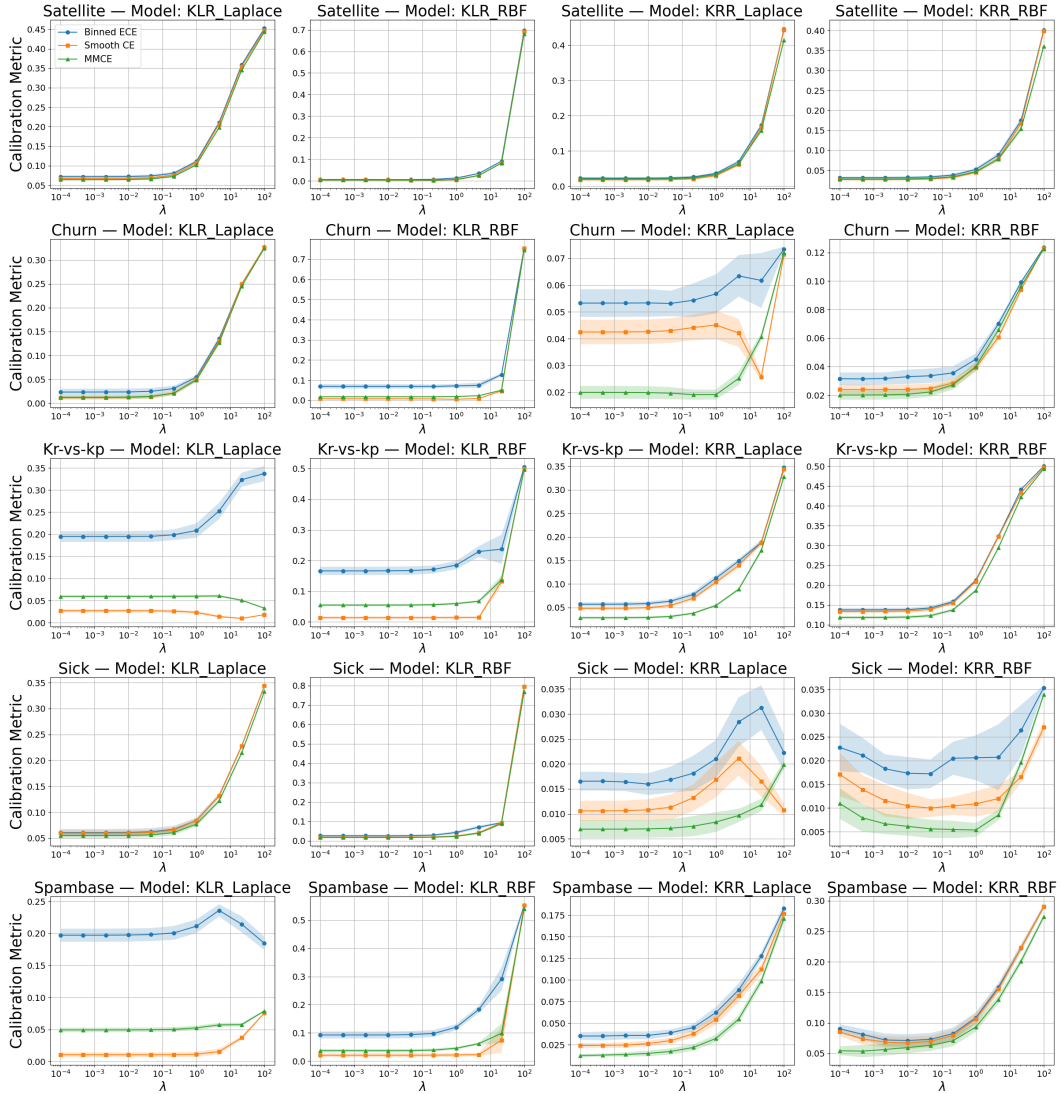


Figure 8: Effect of Sample Size on Calibration Metrics on the real world datasets.